



Asymmetry in carbon cycle feedbacks and transient climate response under positive and negative CO₂ emissions

V. Rachel Chimuka¹ and Kirsten Zickfeld¹

¹Geography Department, Simon Fraser University, Burnaby, BC V5A 1C1, Canada

5 *Correspondence to:* V. Rachel Chimuka (rchimuka@sfu.ca)

Abstract. Most emissions scenarios consistent with limiting warming to well below 2°C above pre-industrial levels rely on carbon dioxide removal to offset residual positive emissions or achieve net-negative emissions. While carbon cycle and climate metrics are well quantified for positive CO₂ emissions, applying the same metrics under negative emissions may over- or underestimate the effectiveness of carbon dioxide removal. This study uses an Earth system model to investigate the asymmetry 10 in carbon cycle feedbacks and climate response under positive and negative CO₂ emissions. To this end, symmetric concentration-driven simulations are initialized from a state at equilibrium with twice the preindustrial CO₂ concentration and run in biogeochimically coupled, radiatively coupled and fully coupled modes. Our results suggest that land and ocean carbon cycle feedbacks are asymmetric. Compared to their respective magnitudes under positive emissions, the concentration-carbon feedback is larger, whereas, the climate-carbon feedback is smaller under negative emissions. Asymmetries in land carbon 15 cycle feedbacks arise from the saturation of the CO₂ fertilization effect and asymmetric temperature and soil respiration responses. Asymmetries in ocean carbon cycle feedbacks are driven by non-linear responses to CO₂ and temperature change, as well as asymmetric ocean circulation responses. Asymmetries in carbon cycle feedbacks propagate onto asymmetry in the Transient Climate Response to Cumulative CO₂ Emissions: a negative CO₂ emission results in greater global mean temperature change than a CO₂ emission of the same magnitude. Our study highlights the need to quantify metrics under negative emissions 20 as reliance on metrics derived from positive emission scenarios may result in inaccurate quantification of the climate response under net negative CO₂ emissions.

1 Introduction

The potential for dangerous climate impacts due to anthropogenic CO₂ emissions prompted the signing of the Paris Agreement, which seeks to limit global warming to well below 2°C above pre-industrial levels, and pursue further efforts to limit it to 25 1.5°C (UNFCCC, 2015). To achieve either climate goal by 2100, substantial emissions cuts are required immediately (United Nations Environment Programme, 2020). Emissions scenarios consistent with the Paris Agreement climate goals heavily rely on artificial carbon dioxide removal (CDR), to not only offset difficult-to-mitigate emissions, but also achieve net-negative emissions, that is, when the amount of CO₂ removed from the atmosphere exceeds the amount of CO₂ added to the atmosphere. Examples of CDR approaches include bioenergy with carbon capture and storage (BECCS), afforestation and reforestation



30 (forestation), direct air capture of CO₂ with carbon capture and storage (DACCs), and ocean alkalinity enhancement, among others (Pathak et al., 2022; Smith et al., 2023).

Emissions scenarios consistent with global climate goals are designed with an assumption of symmetry, that is, removals are applied as negative emissions that offset positive emissions, assuming symmetry in climate outcomes (Zickfeld et al., 2021).

35 For this assumption to be true, the carbon cycle and climate response to a positive CO₂ emission needs to be of equal magnitude and opposite sign to its response to a negative CO₂ emission (Zickfeld et al., 2021). Research shows that this asymmetry does not hold for the carbon cycle, and uncertainties exist for the temperature response, particularly with regards to the sign of the asymmetry (Zickfeld et al., 2016; Zickfeld et al., 2021; Canadell et al., 2021; Koven et al., 2022a, Koven et al., 2022b). Therefore, this study aims to investigate the asymmetry in carbon cycle feedbacks and the climate response under positive and 40 negative CO₂ emissions, focusing on two research questions:

1. To what extent are global land carbon cycle feedbacks asymmetric and what are the mechanisms that drive this asymmetry?
2. To what extent is the temperature response - as quantified through the Transient Climate Response to Cumulative CO₂ Emissions or Removals (TCRE/TCRR metric) - asymmetric, and what drives this asymmetry?

45

Carbon cycling on land and in the ocean regulates atmospheric CO₂ concentration under negative emissions, as it does under positive CO₂ emissions. If negative emissions are implemented but removals remain lower than emissions (net-positive emissions), the land and ocean carbon sinks continue to take up carbon, albeit at a lower rate (Tokarska & Zickfeld, 2015; Jones et al., 2016; Melnikova et al. 2021; Koven et al., 2022a). Once the amount of CO₂ removed from the atmosphere exceeds 50 the amount of CO₂ added to the atmosphere (net-negative emissions), the carbon sinks are expected to weaken further and may reverse, counteracting CDR efforts (Cao & Caldeira, 2010; Tokarska & Zickfeld, 2015; Jones et al., 2016; Melnikova et al., 2021; Zickfeld et al., 2021; Canadell et al., 2021; Koven et al., 2022a). Under net-negative emissions, declining atmospheric CO₂ concentration results in a reversal of carbon sinks to sources (negative concentration-carbon feedback), whereas cooling associated with declining atmospheric CO₂ results in CO₂ uptake (positive climate-carbon feedback) (Schwinger & Tjiputra, 55 Chimuka et al., 2023). The magnitude of these feedbacks determines the extent to which land and ocean carbon cycle responses counteract CDR, and therefore, how effective CDR will be in achieving climate goals (Chimuka et al., 2023).

Quantifying the magnitudes of carbon cycle feedbacks under net-negative emissions, however, is complicated by climate system inertia. The “CDR-reversibility” simulation, which has been commonly used for carbon cycle feedback quantification 60 under negative emissions, is characterized by a CO₂ concentration increase at a rate of 1% per year, followed immediately by a ramp-down at the same rate back to preindustrial CO₂ levels (CDR-MIP: Keller et al., 2014). Studies using these simulations show a lagged carbon cycle response in the ramp-down phase because of climate-system inertia: carbon pools respond to both the decreasing CO₂ concentration and prior increasing CO₂ concentration (Tokarska & Zickfeld, 2015; Zickfeld et al., 2016;



Schwinger & Tjiputra, 2018). This lagged response results in smaller carbon pool changes, and therefore, smaller magnitudes of feedbacks under net-negative emissions relative to positive emissions (Schwinger & Tjiputra, 2018; Chimuka et al., 2023). Chimuka et al., (2023) proposed a novel approach to address climate system inertia and better quantify carbon cycle feedbacks under net-negative emissions. In this approach, climate system inertia was quantified through zero emissions simulations, then subtracted from the CDR-reversibility simulations to isolate the response to negative emissions alone. Findings showed larger feedbacks under negative emissions in the inertia-corrected approach than in the standard approach due to the reduction of climate system inertia effects.

Asymmetries in carbon cycle feedbacks affect the airborne or removal fraction, and thus, asymmetries in the carbon cycle and the associated feedbacks are expected to propagate onto the temperature response. The temperature response to CO₂ emissions is commonly quantified by the Transient Climate response to Cumulative CO₂ Emissions (TCRE) – the ratio of the transient global mean warming to cumulative CO₂ emissions (Matthews et al., 2009). The TCRE is approximately constant over time and across scenarios (Matthews et al., 2009; Gillett et al., 2013; Ehlert et al., 2017; Matthews et al., 2017). Studies exploring the TCRE show that the linear relationship still holds under negative emissions if the temperature response is corrected for ocean thermal and carbon cycle inertia effects as quantified by the zero emissions commitment (Zickfeld et al., 2016; Koven et al., 2022a; Koven et al., 2022b; Sanderson et al., 2025). The TCRE under net-negative emissions is also referred to as the transient climate response to cumulative CO₂ removals (TCRR) (Zickfeld et al., 2021). The magnitude of the TCRE/TCRR asymmetry is highly uncertain (Zickfeld et al., 2016; Zickfeld et al., 2021; Canadell et al., 2021; Koven et al., 2022a, Koven et al., 2022b). Furthermore, the sign of the temperature asymmetry varies across models, with some models exhibiting a larger temperature response under positive emissions and others under negative emissions (Canadell et al., 2021; Koven et al., 2022a; Sanderson et al., 2025).

85

This paper explores the extent to which carbon cycle feedbacks and the transient climate response to CO₂ emissions and removals are asymmetric and the mechanisms behind the asymmetry. Section 2 outlines the experimental design and climate model simulations used as well as the frameworks used to quantify carbon cycle feedback and climate metrics. Section 3 covers the land and ocean carbon cycle feedback and TCRE/TCRR asymmetry results, and the associated mechanisms behind the asymmetry. Understanding the symmetry in carbon cycle feedbacks is integral for determining whether the same metrics, that is, carbon cycle feedback parameters or the TCRE/TCRR, can be applied under both positive and negative emissions.

2 Methods

2.1 Model Description

We use the University of Victoria Earth System Climate Model (UVic ESCM, version 2.10) - a model of intermediate complexity with a horizontal grid resolution of 1.8° (meridional) × 3.6° (zonal) (Weaver et al., 2001; Mengis et al., 2020). The



atmosphere model is a 2D energy-moisture balance model with dynamical wind feedbacks. Atmospheric heat and freshwater are transported through diffusion and advection (Weaver et al., 2001), based on wind velocities prescribed from monthly climatological wind fields from NCAR/NCEP reanalysis data (Eby et al., 2013). This simplified atmosphere model is coupled to a 19-layer 3D ocean general circulation model, including ocean inorganic and organic carbon cycle models, and based on 100 the Geophysical Fluid Dynamics Laboratory (GFDL) Modular Ocean Model version 2 (MOM2; Pacanowski, 1995). The coupled dynamic-thermodynamic sea ice model simulates sea ice dynamics through elastic, viscous, and plastic deformation and flow mechanisms (Weaver et al., 2001).

105 The land surface model, based on the Hadley Centre Met Office Surface Exchange Scheme (MOSES), simulates the terrestrial carbon cycle and is coupled to the Top-Down Representation of Interactive Foliage and Flora including Dynamics (TRIFFID) model which simulates vegetation and soil carbon (Meissner et al., 2003). This model version also includes a permafrost carbon model in the soil module that simulates permafrost carbon through a diffusion-based scheme (MacDougall and Knutti, 2016). Ocean carbon is represented by an inorganic ocean carbon model following the Ocean Carbon Model Intercomparison Protocol 110 (OCMIP), and an NPZD (nutrient, phytoplankton, zooplankton, detritus) model of ocean biology simulating carbon uptake by the biological pump, accounting for phytoplankton light and iron limitations (Keller et al., 2012).

2.2 Model Simulations

115 The model was first integrated under a CO₂ concentration twice that at preindustrial (~560 ppm) for several millennia to achieve an equilibrium state. All other greenhouse gas and aerosol forcings, surface land conditions, and orbital parameters were held at 1850 levels according to the Coupled Model Intercomparison Project Phase 6 (CMIP6) experimental design protocol (Eyring et al., 2016). The solar forcing was set to the 1850–1873 mean and the volcanic forcing was held at its average over 1850–2014, also consistent with the CMIP6 protocol (Eyring et al., 2016).

120 Following the 2xCO₂ spin-up, two idealized symmetric concentration-driven simulations were run. Concentration-driven simulations were chosen in order to expose the land and ocean to the same CO₂ concentrations, facilitating easier separation of concentration-carbon and climate-carbon feedbacks (Gregory et al., 2009; Zickfeld et al., 2011; Schwinger et al., 2014). Both simulations were initialized from a state of equilibrium to quantify the response to positive and negative emissions without climate system inertia effects. In one simulation, atmospheric CO₂ concentration was prescribed to increase at 1% yr⁻¹ until three times the preindustrial CO₂ concentration, and in another the atmospheric CO₂ concentration was prescribed to decline back to preindustrial levels symmetrically (figure 1(a)). In both simulations, it takes roughly 43 years to 125 reach three times the preindustrial CO₂ concentration and preindustrial respectively. We refer to the simulation with increasing atmospheric CO₂ concentration as the positive emissions (PE) simulation, and the simulation with decreasing atmospheric CO₂ concentration as the negative emissions (NE) simulation. Although concentrations are symmetric in both simulations, the diagnosed emissions differ; cumulative positive emissions are approximately 800 PgC, whereas cumulative negative emissions



are 970 PgC (figure 1(c)). The NE simulation includes substantial levels of negative emissions that cannot yet be achieved in
130 the real world (Powis et al., 2023). However, this simulation is symmetric with respect to CO₂ concentrations in the PE simulation, allowing for the quantification of asymmetry in climate-carbon cycle response (figure 1(a)).

To assess the rate-dependence of the asymmetry in the climate-carbon cycle response to positive and negative emissions, we ran additional symmetric concentration-driven simulations derived from the esm-flat10 simulations by Sanderson et al. (2024, 135 2025). The esm-flat10 simulations are emissions-driven simulations with a constant emissions rate of 10 PgC yr⁻¹ for 100 years, reaching cumulative emissions of 1000 PgC. These simulations were designed in line with current annual CO₂ emissions rates and with the goal of diagnosing climate metrics such as the TC_{RE}. As concentration-driven simulations are best suited for the calculation of feedbacks (Arora et al., 2013), we modified the esm-flat10 simulation as follows: First, a fully coupled emissions-driven esm-flat10 simulation was initialized from the an equilibrium state twice the preindustrial CO₂ concentration, 140 then the CO₂ concentration trajectory from that simulation was used to force a concentration-driven simulation, referred to here as the esm-flat10-conc PE simulation (figure 1(a)). In an additional step, the CO₂ trajectory was mirrored over the x-axis to obtain a symmetric trajectory with declining atmospheric CO₂. This CO₂ trajectory was used to run a second simulation, referred to as the esm-flat10-conc NE simulation (figure 1(a)). The rate-dependence was determined by comparing the magnitude and sign of carbon cycle feedbacks and TC_{RE} asymmetry in the 1% yr⁻¹ and esm-flat10-conc simulation pairs. 145 Lastly, we ran all four aforementioned simulations from 2 additional equilibrium states – three times (3xCO₂) and four times (4xCO₂) the preindustrial CO₂ concentration – to test the sensitivity of climate-carbon cycle asymmetry to initial state.

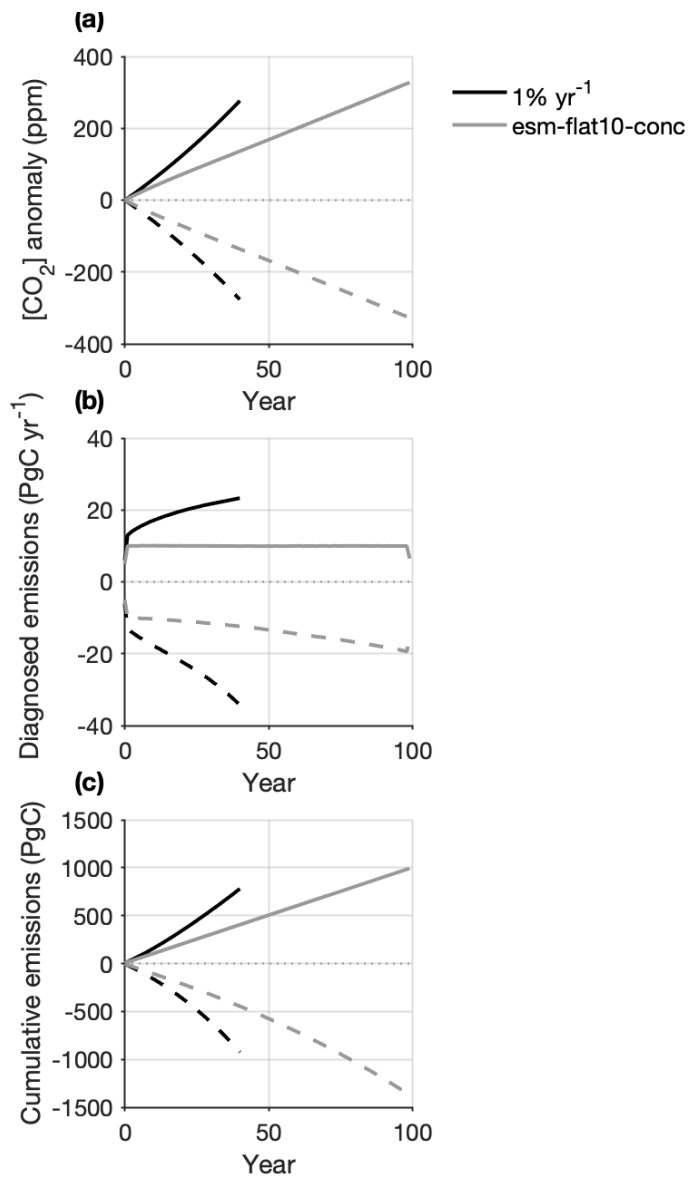


Figure 1: Prescribed atmospheric CO_2 concentration, b. diagnosed annual positive and negative CO_2 emissions, and c. diagnosed cumulative positive and negative CO_2 emissions in the fully coupled (FULL) $1\% \text{ yr}^{-1}$ and esm-flat10-conc positive (PE) and negative (NE) emissions simulations. Solid lines represent the positive emissions run; dashed lines represent the negative emissions run. Panel a is calculated relative to the 2xCO_2 equilibrium state.

All simulations were run in three modes, following the C4MIP protocol for the quantification of carbon cycle feedbacks (Friedlingstein et al., 2006; Arora et al., 2013, 2020; Jones et al., 2016):

155

- Fully coupled mode (FULL): the entire Earth system responds to the specified change in atmospheric CO_2 concentration or CO_2 emissions – in this mode, the land and ocean carbon sinks are subject to changing atmospheric CO_2 concentration and temperature.



160

- Biogeochemically coupled mode (BGC): the land and ocean carbon sinks are subject to changing atmospheric CO₂ concentration but not changing temperature – this is achieved by prescribing a specified time-invariant CO₂ concentration to the radiation module (twice the preindustrial CO₂ concentration for both simulations), while the land and ocean carbon cycle modules see an evolving atmospheric CO₂ concentration.
- Radiatively coupled mode (RAD): the land and ocean carbon sinks are subject to changes in temperature but no change in atmospheric CO₂ concentration – the land and ocean carbon cycle modules see a specified time invariant CO₂ concentration (twice the preindustrial CO₂ concentration in both simulations), while the radiation module sees changing atmospheric CO₂ concentration.

165

Non-CO₂ forcings, including forcings due to other greenhouse gases and aerosols, were held fixed at their preindustrial values.

2.3 Metric Quantification

Asymmetry in global carbon cycle feedbacks was determined by comparing the magnitudes and signs of feedback parameters under positive and negative emissions, evaluated at the end of the simulation. Feedback parameters were quantified following 170 the integrated flux-based feedback framework from Friedlingstein et al. (2006) (see section 2.3.1 below). Feedback parameters under negative emissions were also compared to those from Chimuka et al. (2023), where they were quantified including climate system inertia effects and then corrected for that inertia. The carbon cycle feedback parameters in the esm-flat10-conc symmetric simulations were computed at the same atmospheric CO₂ concentration change, that is, when atmospheric CO₂ concentration change reached 280ppm relative to the spin-up, for ease of comparison to the feedback parameters in the 1% yr⁻¹ simulations.

The temperature asymmetry was assessed in two ways: (1) using a framework that quantifies the TCRE and TCRR, utilizing the Jones & Friedlingstein (2020) framework and (2) using the conventional calculation of the TCRE and TCRR metrics, in which the TCRE was computed as the temperature change for a given amount of cumulative CO₂ emissions, and the TCRR as 180 the temperature change for a given amount of cumulative CO₂ removals. Since the simulations used are concentration-driven, diagnosed emissions were used for the conventional calculation of the TCRE/TCRR. The Jones & Friedlingstein (2020) framework uses the global carbon cycle feedback parameters and the transient climate sensitivity metric from the fully coupled modes to approximate the TCRE and TCRR (see section 2.3.2 below). For validation purposes, the metrics computed from this method were then compared to those calculated using the conventional calculation, evaluated at the end of the simulation. 185 The TCRE and TCRR metrics in the esm-flat10-conc simulations were computed at the same cumulative emissions and removals as in the 1% yr⁻¹ symmetric simulations. The temperature asymmetry was then determined by comparing the magnitudes of the TCRE and TCRR metrics.



2.3.1 Global Carbon Cycle Feedback Framework

190 Carbon cycle feedbacks were quantified using integrated flux-based feedback parameters (Friedlingstein et al., 2006). In the Friedlingstein et al. (2006) feedback framework, the change in land (ocean) carbon due to both CO₂ and climate changes is expressed as the linear sum of the land (ocean) response to the change in the atmospheric CO₂ concentration ΔC_A and surface air temperature ΔT :

[1]
$$\Delta C_L = \beta_L \Delta C_A + \gamma_L \Delta T$$

195 [2]
$$\Delta C_O = \beta_O \Delta C_A + \gamma_O \Delta T$$

The concentration-carbon feedback parameter (β) quantifies the carbon cycle response to changes in CO₂ concentration in units of PgC ppm⁻¹, whereas the climate-carbon feedback parameter (γ) quantifies the carbon cycle response to changes in temperature in units of PgC °C⁻¹ (Friedlingstein et al., 2006). The change in land and ocean carbon due to the increasing atmospheric CO₂ concentration alone is determined using the biogeochemically coupled simulation. In this simulation, the

200 land and ocean only respond to changes in CO₂ concentration, and therefore, this simulation can be used to quantify the concentration-carbon feedback (Friedlingstein et al., 2006). Warming is still observed in this simulation because the water use efficiency of vegetation increases at higher CO₂ concentrations, and changes in albedo, due to shifts in vegetation structure and spatial distribution, result in a small warming effect (Cox et al., 2004; Boer & Arora, 2013; Arora et al., 2013). However, this warming is considered negligible in this feedback framework (Friedlingstein et al., 2006). Assuming $\Delta T = 0$ in Equations

205 [1] and [2], the change in land and ocean carbon is given as:

[3a]
$$\Delta C_L = \beta_L \Delta C_A$$

[4a]
$$\Delta C_O = \beta_O \Delta C_A$$

Equations [3a] and [4a] can then be rearranged to solve for the concentration-carbon feedback parameter β as follows:

$$\beta_L = \frac{\Delta C_L}{\Delta C_A} \quad [3b] \quad \beta_O = \frac{\Delta C_O}{\Delta C_A} \quad [4b]$$

210 The change in land (ocean) carbon due to climate alone is determined using the radiatively coupled simulation. In this simulation, the land and ocean only respond to changes in climate, and therefore, this simulation can be used to quantify the climate-carbon feedback (Friedlingstein et al., 2006). The change in land and ocean carbon is expressed as:

[5a]
$$\Delta C_L = \gamma_L \Delta T$$



[6a]

$$\Delta C_o = \gamma_o \Delta T$$

215 Equations [5a] and [6a] can then be rearranged to solve for the climate-carbon feedback parameter γ as follows:

$$\gamma_L = \frac{\Delta C_L}{\Delta T} \quad [5b] \quad \gamma_o = \frac{\Delta C_o}{\Delta T} \quad [6b]$$

An alternative method for quantifying the change in land (ocean) carbon due to climate change uses the fully coupled and biogeochemically coupled simulations (Arora et al., 2013). We refer to this method as the FULL-BGC method. Here, the change in land (ocean) carbon in the biogeochemically coupled simulation (BGC) is subtracted from that in the fully coupled 220 simulation (FULL) and expressed as the product of the climate-carbon feedback parameter, and the difference between the surface air temperature changes in the two simulations:

$$[7a] \quad \Delta C_L^{FULL} - \Delta C_L^{BGC} = \gamma_L (\Delta T^{FULL} - \Delta T^{BGC})$$

$$[8a] \quad \Delta C_o^{FULL} - \Delta C_o^{BGC} = \gamma_o (\Delta T^{FULL} - \Delta T^{BGC})$$

Equations [7a] and [8a] can then be rearranged to solve for the climate-carbon feedback parameter γ as follows:

$$225 \quad \gamma_L = \frac{\Delta C_L^{FULL} - \Delta C_L^{BGC}}{\Delta T^{FULL} - \Delta T^{BGC}} \quad [7b] \quad \gamma_o = \frac{\Delta C_o^{FULL} - \Delta C_o^{BGC}}{\Delta T^{FULL} - \Delta T^{BGC}} \quad [8b]$$

Feedback parameters were evaluated from equations [3] – [8] for the PE and NE simulations. The feedback parameters for the PE simulation were computed at three times the preindustrial CO₂ level (3xCO₂) and those for the NE simulation were evaluated at the time CO₂ levels return to preindustrial.

2.3.2 Decomposition of Feedback Parameters

230 To better understand the processes driving the asymmetry in the concentration-carbon feedback, we used a framework that decomposes β into vegetation and soil carbon, and the underlying processes, as described in Arora et al. (2020):

$$[9] \quad \beta_L = \frac{\Delta C_L^{BGC}}{\Delta C_A} = \frac{\Delta C_V^{BGC} + \Delta C_S^{BGC}}{\Delta C_A} = \left(\frac{\Delta C_V^{BGC}}{\Delta NPP^{BGC}} \frac{\Delta NPP^{BGC}}{\Delta GPP^{BGC}} \frac{\Delta GPP^{BGC}}{\Delta C_A} \right) + \left(\frac{\Delta C_S^{BGC}}{\Delta R_h^{BGC}} \frac{\Delta R_h^{BGC}}{\Delta LF^{BGC}} \frac{\Delta LF^{BGC}}{\Delta C_A} \right) \\ = \tau_{cveg\Delta} \text{CUE}_\Delta \frac{\Delta GPP^{BGC}}{\Delta C_A} + \tau_{csoil\Delta} \frac{\Delta R_h^{BGC}}{\Delta LF^{BGC}} \frac{\Delta LF^{BGC}}{\Delta C_A}$$

The sensitivity of vegetation carbon to changes in CO₂ concentration can be decomposed to a product of the residence time of 235 vegetation carbon $\tau_{cveg\Delta}$, the carbon use efficiency (CUE) – proportion of GPP that is turned into NPP – and a measure of the



CO₂ fertilization effect. The sensitivity of soil carbon to changes in CO₂ concentration can be decomposed to a product of the residence time of soil carbon $\tau_{csoil\Delta}$, the change in the soil respiration rate per unit change in the leaf litter flux, and the sensitivity of the leaf litter flux to changes in CO₂ concentration. All changes in variables were calculated relative to the 2xCO₂ (twice the preindustrial CO₂ concentration) equilibrium state.

240 2.3.3 TCRE Framework

The Transient Climate Response to Cumulative CO₂ Emissions (TCRE) is a near-linear relationship between transient warming and cumulative CO₂ emissions (Matthews et al., 2009). According to the Jones & Friedlingstein (2020) framework, the TCRE can be expressed as the product of the climate sensitivity parameter (α) and the cumulative airborne fraction (AF) as follows:

$$[10] \quad \text{TCRE} = \alpha \left(\frac{\text{AF}}{k} \right)$$

245 where k is a constant to account for unit conversion ($k = 2.12 \text{ PgC ppm}^{-1}$)

The cumulative airborne fraction can be expressed in a form with individual carbon cycle feedback parameters as follows:

$$[11] \quad \text{AF} = \frac{k}{k + \beta + \alpha\gamma}$$

Substituting equation [11] into [10] gives the TCRE as:

$$[12] \quad \text{TCRE} = \frac{\alpha}{k + \beta + \alpha\gamma}$$

250 The climate sensitivity parameter (α) and AF (as calculated from equation [11]) were evaluated at three times the preindustrial CO₂ level (3xCO₂) for PE simulation, and at the time CO₂ levels return to preindustrial for the NE simulation, consistent with the quantification time points for feedback parameters.

3 Results

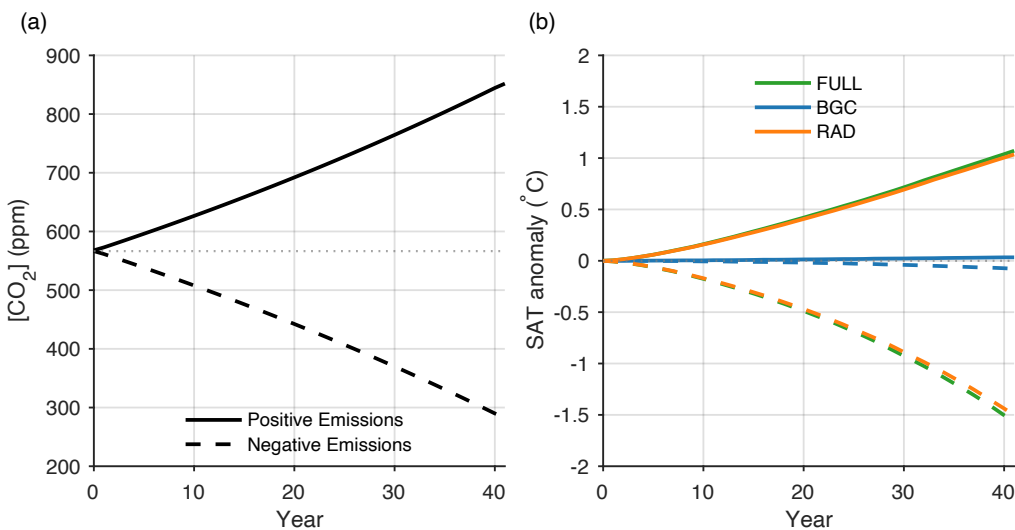
Our results section focuses on carbon cycle feedback and TCRE asymmetry under positive and negative emissions. Sections 255 3.1 – 3.2 explore the carbon cycle feedback asymmetry from the 1% yr⁻¹ simulation pairs, and the rate- and state-dependence of these results. Section 3.3 focuses on TCRE asymmetry and its rate- and state-dependence.

3.1 Physical Climate Response

The prescribed atmospheric CO₂ concentration profiles are symmetric by design, with a change in CO₂ concentration of ~280 ppm (figure 2(a)). However, the surface air temperature shows considerable asymmetry in the FULL and RAD modes (figure 260 2(b)). In both modes, the surface air temperature decreases more in the NE simulation relative to the PE simulation by approximately 0.5°C (figure 2(b)). This occurs because of the logarithmic relationship between radiative forcing and atmospheric CO₂ concentration in the UVic ESCM, which leads to a greater response to declining than rising CO₂ levels (Eby



et al., 2013). The BGC mode for both simulations sees small temperature changes (figure 2(a, b)) that result from biophysical responses to changes in CO₂ concentration, such as changes in the evapotranspiration flux and surface albedo (Cox et al., 2004; 265 Boer & Arora, 2013; Arora et al., 2013. The difference between the FULL and RAD temperature responses is also due to these biophysical responses.



270 **Figure 2: a. Prescribed atmospheric CO₂ concentration and b. surface air temperature (SAT) change in the fully coupled (FULL), biogechemically coupled (BGC) and radiatively coupled (RAD) positive (PE) and negative (NE) emissions simulations relative to the 2xCO₂ equilibrium state.**

3.2 Quantifying Carbon Cycle Feedback Asymmetry

3.2.1 Land Carbon Change Asymmetry in the FULL Mode

Despite symmetry in the atmospheric CO₂ concentration profiles in Figure 2(a), the land carbon pool exhibits asymmetry for all 3 modes (figure 3(a)). Asymmetry in carbon pools is determined by comparing the carbon change at the end of the PE and 275 NE simulations. If the carbon change is greater under negative (positive) emissions, then the asymmetry is positive (negative). The FULL mode exhibits the greatest asymmetry of all 3 modes, with the land gaining 70.7 PgC under positive emissions and losing 154 PgC under negative emissions (figure 3(a)). This results in a positive asymmetry of roughly 83 PgC. The sign of the asymmetry is the same for both vegetation and soil carbon pools, with the vegetation carbon pool exhibiting the larger positive asymmetry (PE: 35.3 PgC; NE: -90.5 PgC) (figure 3(c, d)).

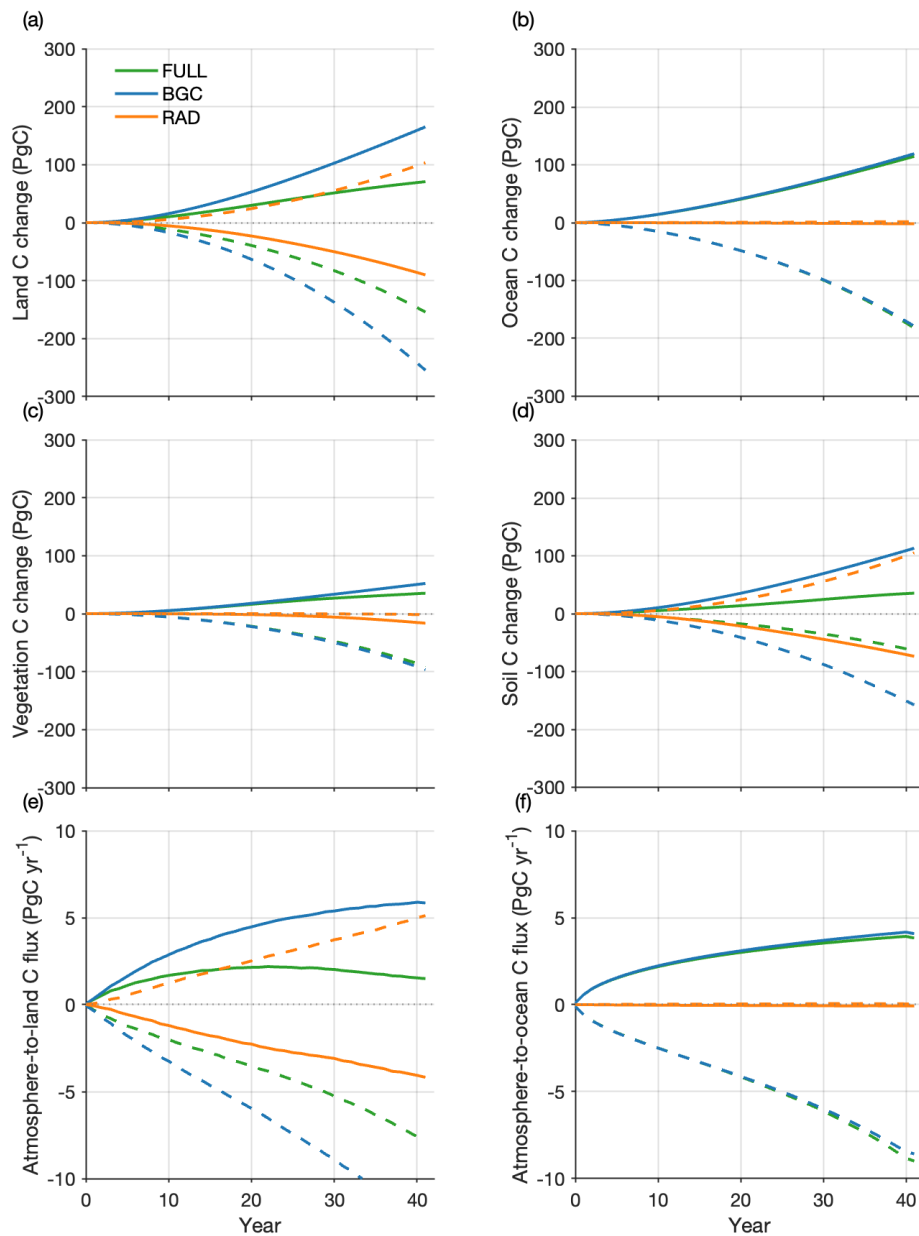


Figure 3: a. Land b. ocean c. vegetation and d. soil carbon pool changes as a function of time for the fully coupled (FULL), biogeochemically coupled (BGC) and radiatively coupled (RAD) modes of the positive (PE) and negative (NE) emissions simulations. Solid lines represent the PE run; dashed lines represent the NE run. Panels a - d are calculated relative to the 2xCO₂ equilibrium state. The atmospheric carbon fluxes are also shown in panels e and f.



The land carbon balance determines the change in the land carbon pool. Under positive emissions, the CO₂ fertilization effect drives carbon uptake; photosynthesis is enhanced under increasing CO₂ concentration, increasing NPP (figure 4(a)). Warming enhances soil respiration, but the soil respiration remains lower than NPP, leading to land carbon sequestration. Under negative 290 emissions, NPP is consistently lower than soil respiration largely because of the asymmetry in NPP under increasing and declining CO₂ concentrations (figure 4(a)). The saturation of NPP at higher atmospheric CO₂ concentration results in a smaller enhancement of NPP with increasing CO₂ concentration and a larger reduction in NPP with decreasing CO₂ concentration. Soil respiration is also asymmetric: with cooling decreasing soil respiration more than warming increases soil respiration 295 (figure 4(a)), consistent with the asymmetric temperature response in the FULL mode (figure 2(b)). As NPP decreases faster than soil respiration under negative emissions, the land loses CO₂ to the atmosphere.

3.2.2 Land Carbon Change Asymmetry in the BGC Mode

Isolating the component of the land carbon response due to changes in atmospheric CO₂ concentration only, our results 300 consistently show asymmetry in land carbon change (figure 3(a)). In the PE simulation, the land sequesters about 165 PgC, whereas the land in the NE simulation loses 255 PgC (figure 3(a)). This results in a positive asymmetry of 90 PgC. The sign and magnitude of the asymmetry is similar for the vegetation and soil carbon pools (figure 3(c, d)).

Similar to the FULL mode, the CO₂ fertilization effect promotes carbon uptake under positive emissions (figure 4(b)). However, NPP increases faster in the absence of significant climate change. The increase in soil respiration in the BGC mode 305 is mainly driven by increasing soil carbon stocks. The increase in soil respiration is, however, smaller than the increase in NPP, promoting carbon uptake. Under negative emissions, both NPP and soil respiration decrease more than they increase under positive emissions due to the asymmetry in the responses of NPP and soil carbon change to changes in CO₂ concentration (figure 4(b)). NPP declines faster than soil respiration, and the land releases CO₂ to the atmosphere.

The vegetation and soil carbon components of the response to CO₂ (figure 4(c, d)) can be decomposed into three parts according 310 to Arora et al. (2020) to better understand the mechanisms driving the observed asymmetries. The asymmetry in the vegetation component is largely driven by increased sensitivity of NPP to CO₂ concentration change and longer vegetation carbon residence time under negative emissions (Table S1.1). In the soil component, the response of the litter flux to changes in CO₂ concentration is larger under negative emissions, dominating the soil carbon asymmetry (Table S1.1).

3.2.3 Land Carbon Change Asymmetry in the RAD Mode

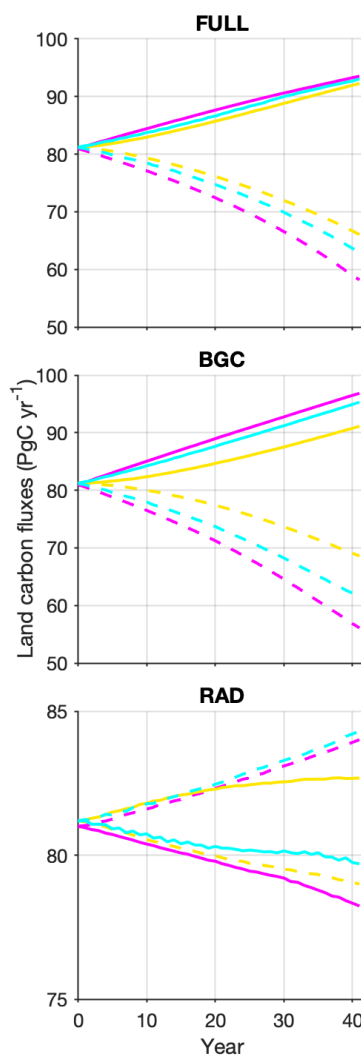
Through the RAD mode, which shows the land carbon response to climate change, our results show the least asymmetry of all 315 three modes (figure 3(a)). The land loses 90.1 PgC in the PE simulation and gains 103 PgC in the NE simulation, resulting in a positive asymmetry of 12.9 PgC (figure 3(a)). The sign of the asymmetry in the soil carbon pool is consistent with that for the land carbon pool, with the soil carbon pool losing 73.7 PgC under positive emissions and gaining 105.1 PgC under negative



emissions (figure 3(d)). The asymmetry in the vegetation carbon pool, however, is small and negative (figure 3(c)) and by the end of the simulation, the vegetation carbon pools in both simulations lose carbon (PE: -1.8PgC; NE: -16.4 PgC) (figure 3(c)).

320

In the absence of the CO₂ fertilization effect, NPP declines with warming, primarily due to an increase in plant respiration, while soil respiration increases with warming under positive emissions. As soil respiration is greater than NPP, the land releases CO₂ into the atmosphere (figure 4(c)). Under negative emissions, NPP increases as plant respiration decreases with cooling, whereas, soil respiration declines (figure 4(c)). NPP remains greater than soil respiration, promoting carbon sequestration.



325
Figure 4: Land carbon fluxes for the three modes are shown. NPP = net primary productivity, LLF = leaf litter flux and SR = soil respiration. Fully coupled (FULL); biogeochemically coupled (BGC); radiatively coupled (RAD). Solid lines represent the positive (PE) emissions run; dashed lines represent the negative emissions (NE) run. Note the difference in the vertical scale of the RAD panel (last panel).



330 **3.2.4 Ocean Carbon Change Asymmetry in the FULL, BGC and RAD modes**

The ocean carbon pool exhibits considerable positive asymmetry in the FULL and BGC modes (figure 3(b)), losing more carbon under negative emissions than it gains under positive emissions, consistent with previous literature (Zickfeld et al., 2021). The magnitude of the positive asymmetry is similar for the FULL and BGC modes, whereas the RAD mode shows small negative asymmetry (PE: -2 PgC; NE: 1.7 PgC) (figure 3(b)).

335

In the FULL mode, the overall response to CO₂ and temperature changes combined results in a larger flux of CO₂ out of the ocean under negative emissions than the flux into the ocean under positive emissions (figure 3(f)) (Zickfeld et al., 2021). This asymmetric ocean carbon response is partly driven by the imbalance between atmospheric CO₂ concentration and the partial pressure of CO₂ in the surface ocean, which results in a larger flux of CO₂ out of the ocean under negative emissions than the 340 flux into the ocean under positive emissions (figure 3(f), see supplementary figure S1.1). In addition, there is a non-linear inverse relationship between the ocean's ability to buffer additional CO₂ and the partial pressure of CO₂ in the surface ocean (Chapin and Eviner, 2014). With increasing partial pressure of CO₂ in the surface ocean, the buffer capacity is expected to decline less than it increases with decreasing partial pressure of CO₂. This relationship favours a greater loss of ocean carbon 345 under negative emissions than gain under positive emissions. Non-linearities related to ocean circulation and CO₂ solubility in seawater also drive the observed ocean carbon asymmetry (Zickfeld et al., 2021). The Atlantic meridional overturning circulation (AMOC) strengthens more under negative emissions than it weakens under positive emissions. Under positive emissions, a weaker AMOC drives less carbon into the ocean due to weaker vertical mixing. Under negative emissions, a stronger AMOC drives a larger flux out of the ocean as carbon is more efficiently mixed upwards and released to the atmosphere (see supplementary figure S1.2). The combined effect of the CO₂ concentration imbalance at the atmosphere-ocean 350 interface and the AMOC changes is partly counteracted by the effect of CO₂ solubility changes. The response of CO₂ solubility to changes in ocean temperature is non-linear (Duan and Sun, 2003), that is, the solubility of CO₂ in the surface ocean increases more with cooling than it decreases with warming, resulting in a greater enhancement of carbon uptake capacity under negative emissions than reduction under positive emissions.

355 The ocean carbon cycle response to CO₂ and temperature changes is isolated in the BGC and RAD modes respectively. In the BGC mode, the imbalance between atmospheric CO₂ concentration and the partial pressure of CO₂ in the surface ocean partly determines the magnitude and direction of the atmosphere-ocean CO₂ flux. This imbalance is larger under negative emissions, resulting in a larger flux of CO₂ out of the ocean under negative emissions than the flux into the ocean under positive emissions (figure 3(f), see supplementary figure S1.1). Non-linearities in buffer capacity (Chapin and Eviner, 2014) also favour greater 360 loss of greater loss of ocean carbon under negative emissions than gain under positive emissions from the ocean's surface, as in the FULL mode.



In the RAD mode, the flux out of the ocean under positive emissions is only slightly larger than that into the ocean under negative emissions (figure 3(f)) because of two counteracting effects. The AMOC strengthens more under negative emissions than it weakens under positive emissions, driving a larger flux out of the ocean under negative emissions than the flux into the ocean under positive emissions (see supplementary figure S1.2). The effect of AMOC changes is dominated slightly by the non-linearity in the response of CO₂ solubility to changes in ocean temperature (Duan and Sun, 2003): the solubility of CO₂ in the surface ocean increases more with cooling than it decreases with warming, increasing the carbon uptake capacity of the ocean under negative emissions more than it reduces it under positive emissions.

3.2.5 Asymmetry in carbon cycle feedback parameters

The land and ocean carbon response to atmospheric CO₂ concentration gives rise to the negative concentration-carbon feedback: increasing atmospheric CO₂ concentration promotes land and ocean carbon uptake, acting to draw down CO₂ from the atmosphere, whereas declining CO₂ concentration reverses both carbon sinks, releasing CO₂ to the atmosphere. On the other hand, the land and ocean carbon response to temperature change give rise to the positive land climate-carbon feedback, in which warming causes land and ocean carbon loss, while cooling promotes carbon gain. The concentration-carbon feedback parameter (β) is quantified from the BGC mode as the land or ocean carbon change per unit change in atmospheric CO₂ concentration (units: PgC ppm⁻¹). The climate-carbon feedback (γ), computed from the RAD mode, quantifies the land or ocean carbon change per unit change in surface air temperature (units: PgC °C⁻¹). These feedbacks were quantified using the carbon cycle feedback framework in Section 2.3.1 and are shown in Figure 5.

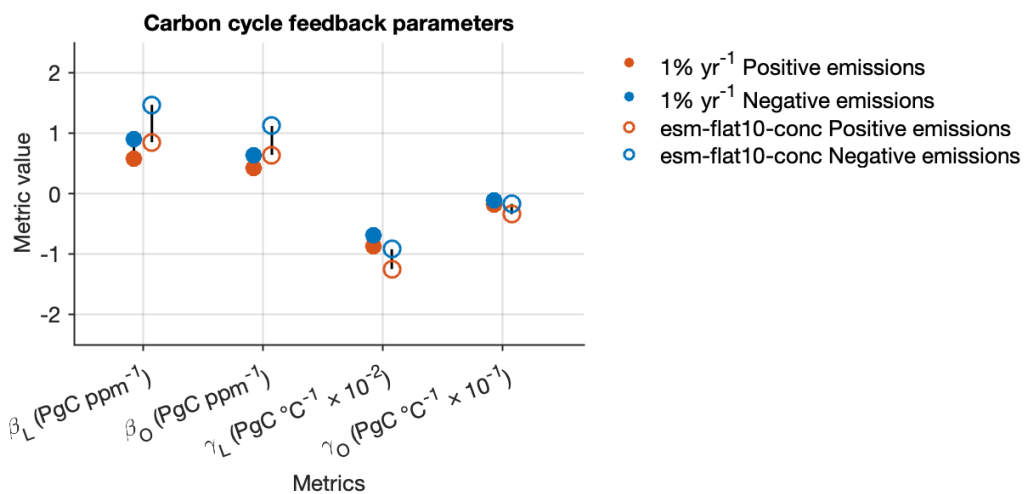


Figure 5: Carbon cycle feedback parameters quantified at the time the CO₂ concentration reaches 3xCO₂ (three times the preindustrial CO₂ level) for positive emissions (PE) and preindustrial for negative emissions (NE), respectively for the 1% yr⁻¹ and esm-flat10-conc simulation pairs. Feedback parameters under negative emissions are positive for land or ocean carbon loss and negative for land or ocean carbon gain, opposite to the sign convention for feedbacks under positive emissions. Note that the γ_O values are scaled up by one order of magnitude and the γ_L values are scaled up by two orders of magnitude to plot them on the same axis as the β values.



Carbon cycle feedback parameters differ under positive and negative emissions. The land and ocean β are larger under negative emissions than under positive emissions. Conversely, the land and ocean γ are larger under positive emissions. The asymmetry in γ is partly influenced by the asymmetric temperature response. A larger temperature change under negative emissions means a greater denominator in the gamma calculation (Section 2.3.1), favouring a smaller γ under negative emissions. This is only
390 slightly countered by the small positive asymmetry in the land and ocean carbon pools, which favours a larger γ under negative emissions.

3.2.6 Rate- and state-dependence of asymmetry in carbon cycle feedback parameters

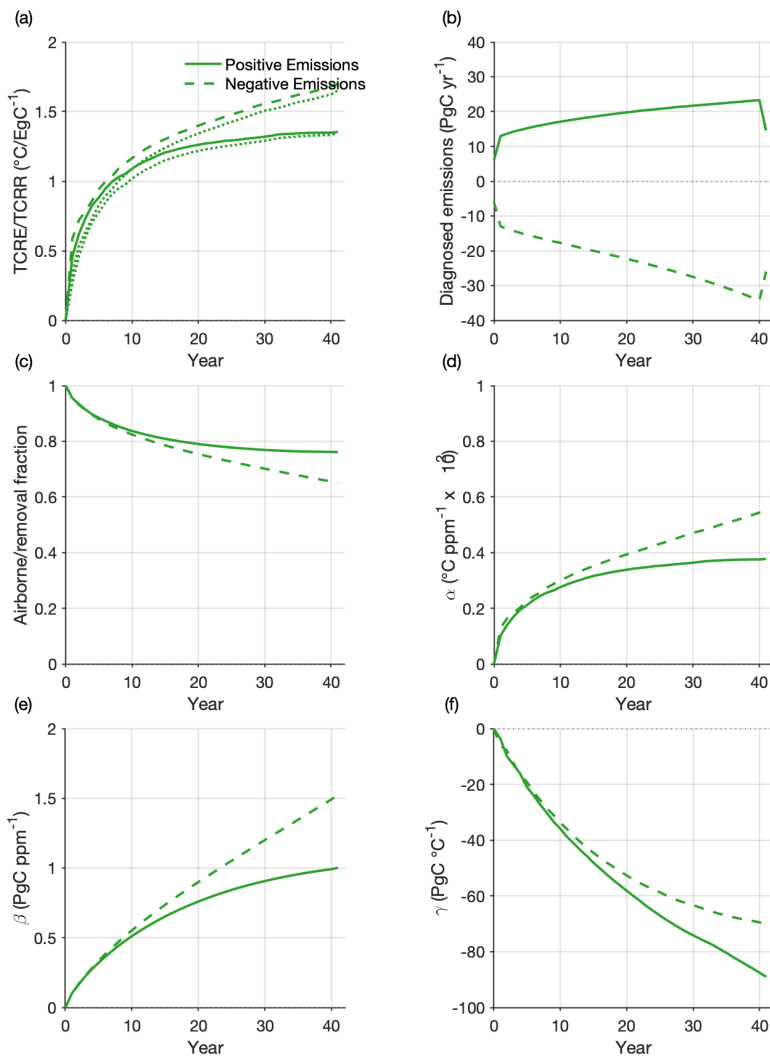
The rate-dependence of carbon cycle feedback parameter asymmetry is determined by comparing feedback parameters calculated with the 1% yr^{-1} simulations with those calculated using the esm-flat10-conc simulations. In the esm-flat10-conc
395 PE and NE simulations, CO_2 concentrations evolve at a lower rate, reaching 3x CO_2 and preindustrial respectively roughly 40 years after the 1% yr^{-1} simulations (figure 1(a)). Both feedbacks are smaller at higher rates of CO_2 change (figure 5). In addition, the magnitude of the asymmetry exhibits rate-dependence: the higher the rate of CO_2 change, the smaller the asymmetry. The sign of the asymmetry, however, is robust. The land and ocean β are larger under negative emissions whereas, land and ocean γ are larger under positive emissions, independent of rate.

400

In addition to rate-dependence, we investigated whether carbon cycle feedback parameter asymmetry is sensitive to the initial state (figure S1.3). Using 1% yr^{-1} PE and NE simulations initialized from 2x CO_2 , 3x CO_2 and 4x CO_2 equilibrium states, we found that for land and ocean β , the magnitude of the asymmetry decreased with increasing initial CO_2 concentration, while
405 the sign of the asymmetry showed no sensitivity to initial state. Findings for land and ocean γ were more complex, with both the magnitude and sign of the asymmetry showing no clear or consistent pattern (figure S1.3).

3.3 Quantifying TCRE asymmetry

In this section we explore how the asymmetry in carbon cycle feedbacks propagates onto asymmetry in the Transient Climate Response to Cumulative CO_2 Emissions and Removals (TCRE/TCRR) using the fully coupled modes of the 1% yr^{-1} and esm-flat10-conc simulation pairs. We quantify this asymmetry using the Jones & Friedlingstein (2020) framework (see Section
410 2.3.1). For validation purposes, we compare this to the conventional TCRE/TCRR calculations ($\Delta T/\text{CE}$ and $\Delta T/\text{CR}$), where ΔT is the surface air temperature anomaly and CE (CR) is cumulative emissions (removals). Figure 6(a) shows that the Jones & Friedlingstein (2020) framework generally approximates the TCRE reasonably well under both positive and negative emissions, especially towards the end of the simulation.



415 **Figure 6: a. Transient climate response to cumulative CO_2 emissions and removals. Solid and dashed lines – calculated from the**
 Jones & Friedlingstein (2020) framework for the positive (PE) and negative emissions (NE) runs respectively; dotted lines – direct
 calculation (ratio of global mean temperature change to cumulative emissions or removals) b. diagnosed positive or negative
 420 emissions c. airborne fraction for positive emissions; removal fraction for negative emissions d. climate sensitivity parameter α e.
 concentration-carbon feedback parameter β f. climate-carbon feedback parameter γ under positive and negative emissions. The
 carbon cycle feedbacks represent the total sensitivity of the carbon pools (land plus ocean carbon) to changes in CO_2 concentration
 and temperature.

The TCRE/TCRR exhibits asymmetry: the cooling per unit negative emission is larger than the warming per unit positive emission (figure 6(a)). The asymmetry in the TCRE is positive, with the TCRE larger under negative emissions levels ($1.63 ^{\circ}\text{C EgC}^{-1}$) than under positive emissions ($1.37 ^{\circ}\text{C EgC}^{-1}$), consistent with Zickfeld et al. (2021). The Jones & Friedlingstein (2020) framework allows us to decompose the TCRE into three contributing factors - the airborne or removal fraction (AF/RF), the climate sensitivity (α), and the carbon cycle feedback parameters (β, γ), (see section 2.3.2) – and quantify the asymmetry



in each to determine the process driving TCRE asymmetry. The airborne fraction (AF) is defined as the fraction of emissions that remain in the atmosphere, whereas, the removal fraction (RF) shows the fraction of removals that stay out of the atmosphere. The RF and AF are initially equal, then the RF decreases at a greater rate than the AF until it is smaller by 0.11
430 (figure 6(c)). The asymmetry in the AF/RF is negative because diagnosed negative emissions are larger than diagnosed positive emissions (figure 6(b)).

Climate sensitivity (α), a measure of the transient temperature response to changing CO₂ concentration, increases at a greater rate under negative emissions, resulting in an asymmetry of 0.0017 °C ppm⁻¹ (figure 6(d)). This positive asymmetry occurs
435 because the surface air temperature anomaly is larger under negative emissions (figure 2(b)). Under negative emissions, a larger AF favours a smaller TCRE in the PE simulation whereas, a larger α favours a larger TCRE. Here, the TCRE is larger in the NE simulation (figure 6(a)), implying that α is the dominant influence on the sign of the TCRE.

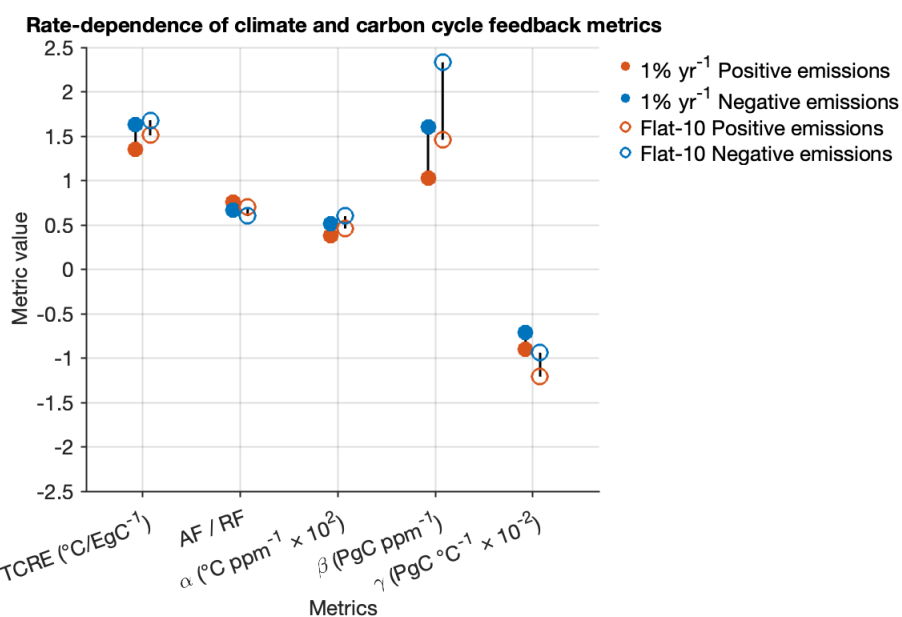
The AF/RF can also be computed using α and the two carbon cycle feedback parameters β and γ (see section 2.3.1) (Jones &
440 Friedlingstein, 2020). A larger β acts to reduce AF (RF) through land and ocean carbon uptake (loss), a larger γ acts to increase AF (RF) through land and ocean carbon loss (uptake). β increases at a greater rate under negative emissions, and by the end of the simulation, the asymmetry is positive, with a β of 1.6 PgC ppm⁻¹ in the PE simulation and 1.03 PgC ppm⁻¹ in the NE simulation (figure 6(e)). A larger β acts to reduce the TCRE, favouring a smaller TCRE in the NE simulation. γ decreases faster under positive emissions, and by the end of the simulation, γ is 21.9 PgC °C⁻¹ larger in magnitude (negative
445 asymmetry) (figure 6(f)). This occurs because of both larger combined land and ocean carbon loss and surface air temperature change in the NE simulation. A larger γ (in magnitude) favours a larger TCRE in the PE simulation.

3.3.1 Rate- and state-dependence of TCRE asymmetry

The TCRE asymmetry analysis was repeated with esm-flat10-conc simulations to test the rate-dependence of TCRE asymmetry. The magnitude and sign of the TCRE asymmetry are broadly consistent with results in the 1% yr⁻¹ simulations:
450 the sign of the TCRE asymmetry is robust, with the magnitude exhibiting little rate-dependence (figure 7). Out of the three contributors to TCRE asymmetry, the carbon cycle feedbacks show the greatest rate-dependence. As described in Section 3.1.6, the sign of the asymmetry in feedbacks parameters is robust, whereas the magnitude of the asymmetry in carbon cycle feedback parameters is smaller with higher rates of CO₂ change. An additional insight from Figure 7 is the relatively large asymmetry observed in β compared to the asymmetry in the TCRE. According to the Jones & Friedlingstein (2020) framework
455 (Section 2.3.3), the effect of β on the TCRE counteracts the combined effects of α and γ . The TCRE asymmetry is, therefore, small because of partial cancellation of asymmetry in these contributors.



460 In addition to rate-dependence, we investigated the state-dependence of the TCRE (figure S1.4). The sign of the TCRE asymmetry is state independent, while the magnitude of the asymmetry exhibits little state-dependence, decreasing with higher initial states. Overall, the sign of the TCRE asymmetry is independent of rate and initial state. The magnitude of the asymmetry shows little rate- and state-dependence, increasing with higher rates and decreasing with higher initial states.



465 **Figure 7: Rate-dependence of climate and carbon cycle feedback metrics in the fully coupled 1% yr^{-1} and esm-flat10-conc positive (PE) and negative emissions (NE) simulations. Metrics shown include: the transient climate response to cumulative CO_2 emissions and removals (TCRE/TCRR), airborne fraction for positive emissions (AF) and removal fraction for negative emissions (RF), climate sensitivity parameter α , concentration-carbon feedback parameter β and climate-carbon feedback parameter γ . The carbon cycle feedbacks represent the total sensitivity of the carbon pools (land plus ocean carbon) to changes in CO_2 concentration and temperature. Vertical black lines depict the asymmetry under positive and negative emissions.**

470 4 Discussion

Carbon cycle feedbacks under negative emissions have previously been quantified from CDR reversibility simulations (CDR-MIP: Keller et al., 2014), in which a phase of CO_2 decline (negative emissions) immediately follows a phase of CO_2 increase (positive emissions). In these studies, the magnitudes of both feedbacks are smaller under negative emissions because of climate system inertia (Schwinger et al., 2018; Chimuka et al., 2023). Although other studies using preindustrial as the 475 reference year for quantifying feedbacks under negative emissions show that both feedbacks become larger under negative emissions, they also show the same lagged carbon pool response (Melnikova et al., 2021; Asaadi et al., 2024). Chimuka et al. (2023) proposed an approach to correct for climate system inertia and found a larger climate-carbon feedback and smaller concentration-carbon feedback under negative emissions, inconsistent with our findings here. This discrepancy may arise due to differences in simulation configuration, non-linearity and irreversible vegetation distribution changes (Chimuka et al., 2023).



480 The benefit of the novel approach used in this study is that it eliminates climate system inertia by prescribing both CO₂ trajectories from the same equilibrium state, allowing for a more accurate quantification of carbon cycle feedbacks under positive and negative emissions.

485 The temperature response in the FULL mode, as quantified by the TCRE, is asymmetric: the TCRE is larger under negative emissions than under positive emissions, consistent with a previous study that used simulations with symmetric emissions trajectories (Zickfeld et al., 2021). The sign of the temperature asymmetry is generally uncertain in the literature; some models exhibit positive asymmetry (consistent with our findings here) while others exhibit negative asymmetry (Zickfeld et al., 2016; Canadell et al., 2021; Zickfeld et al., 2021; Koven et al., 2022). The three contributing factors to the TCRE – the airborne or removal fraction (AF/RF), the climate sensitivity (α), and the carbon cycle feedback parameters (β, γ) – are also all 490 asymmetric. Under negative emissions, the RF is smaller than the AF, favouring a smaller TCRE under negative emissions. However, α is larger under negative emissions, favouring a larger TCRE under negative emissions. Given that the TCRE is larger under negative emissions, this shows that α is the more dominant influence on the sign of the TCRE than the AF/RF is. Overall, the carbon cycle feedback asymmetry favours more carbon loss per negative emission than carbon gain per positive 495 emission, whereas, the temperature asymmetry favours more cooling per negative emission than warming per positive emission, countering the carbon cycle feedback asymmetry.

500 In the real world, a decline in CO₂ concentration is expected to follow a transient state of positive or zero emissions, rather than an equilibrium state. In this case, carbon cycle feedbacks and the TCRE would be asymmetric with smaller metrics under negative emissions as shown through the CDR-reversibility simulations in earlier studies (Zickfeld et al., 2016; Chimuka et al., 2023). However, the benefit of the experimental design we propose here is that there are no climate system inertia effects (both simulations are prescribed from the same equilibrium state), allowing for a positive and negative emissions to be applied from equilibrium. We chose to initialize our simulations from equilibrium, with the 2xCO₂ equilibrium state used as default, rather than real world conditions. Findings show that the sign of the concentration-carbon feedback is robust, with the magnitude showing little state-dependence. (Figure S1.3). However, the magnitude and sign of the climate-carbon feedback 505 asymmetry both exhibit state-dependence, with neither showing a consistent pattern (Figure S1.3). Our results also suggest that the signs of the carbon cycle feedback and TCRE asymmetries are independent of rate, with only the magnitude of the carbon cycle feedback asymmetry exhibiting notable rate-dependence. The TCRE asymmetry exhibits little state-dependence, and the sign of the asymmetry is robust. These findings align with previous research that carbon-cycle feedbacks exhibit state- and scenario-dependence (Gregory et al., 2009; Boer & Arora, 2010; Zickfeld et al., 2011; Hajima et al., 2014), while the 510 TCRE itself remains largely invariant (Matthews et al., 2009).

The model used here (UVic ESCM) couples the climate and carbon cycles, allowing for the computation of carbon cycle feedbacks, and can run climate model simulations at low computational cost. However, the atmospheric model is a simple



energy-moisture balance model, and therefore, is missing several key physical feedbacks such as the cloud feedback and lapse rate feedback, among others. Inclusion of these feedbacks would benefit our TCRE analysis by accounting for asymmetries in the physical response that are currently missing from our results. Furthermore, the model is known to show a stronger saturation of radiative forcing compared to other earth system models, implying that the warming trends here may be smaller compared to other earth system models (Koven et al., 2022). The UVic ESCM also does not explicitly account for the nitrogen cycle on land and its coupling to the carbon cycle. Under positive emissions, nitrogen limitation acts to constrain the CO₂ fertilization effect, which decreases the magnitude of the concentration-carbon feedback (Friedlingstein & Prentice, 2010). Nitrogen remineralization makes nitrogen more bioavailable, fertilizing plants, and reducing the magnitude of the positive climate-carbon feedback (Friedlingstein & Prentice, 2010). Under negative emissions, we expect that the CO₂ fertilization effect would be weakened further, causing further carbon loss due to the concentration-carbon feedback, whereas, nitrogen remineralization would decline as surface air temperature declines, reducing carbon gain due to the climate-carbon feedback.

525 5 Conclusions

Using idealized simulations with symmetric changes in atmospheric CO₂, our results show that carbon cycle feedbacks are asymmetric. Compared to their respective magnitudes under positive emissions, the concentration-carbon feedback parameter is larger under negative emissions whereas, the climate-carbon feedback is smaller. The asymmetry in the concentration-carbon feedback is related to the saturation of the CO₂ fertilization effect, whereas the asymmetry in the climate-carbon feedback is 530 partly related to asymmetric temperature and soil respiration responses. Asymmetries in ocean carbon cycle feedbacks are driven by asymmetries in the disequilibrium in CO₂ concentration at the atmosphere-ocean interface, asymmetric ocean circulation responses and non-linearities in CO₂ solubility and buffer capacity. The combined behaviour of both carbon cycle feedbacks under negative emissions results in carbon release to the atmosphere, reducing the effectiveness of carbon dioxide removal at decreasing CO₂ levels. Although the magnitude of the carbon cycle feedback asymmetry exhibits rate-dependence, 535 the sign is robust. The state-dependence is, however, more complex. The magnitude of the concentration-carbon feedback asymmetry is sensitive to initial state, while the sign of the asymmetry is robust. However, the magnitude and sign of the climate-carbon feedback asymmetry shows no clear or consistent pattern. Our findings show that the TCRE is asymmetric, that is, larger under negative emissions than under positive emissions, and that the contributing factors (airborne/removal fraction, climate sensitivity and carbon cycle feedback metrics) are all asymmetric. Out of the three factors, the climate 540 sensitivity has the greatest influence on the sign of the TCRE asymmetry. The magnitude and sign of the TCRE asymmetry show little to no rate- or state-dependence.

This study builds on previous work on the climate and carbon cycle response to positive and negative emissions, providing 545 insights into carbon cycle feedback and TCRE asymmetry and the associated driving mechanisms. We also propose a novel experimental design that eliminates climate system inertia effects, allowing for more accurate quantification of carbon cycle



feedbacks under negative emissions. Our results are more variable for the climate-carbon feedback asymmetry as compared to the concentration-carbon feedback asymmetry. The concentration-carbon feedback depends on CO₂ concentration, which is symmetric in our study, whereas, the climate-carbon feedback is more closely tied to the temperature response, which exhibits asymmetry itself. Exploring climate-carbon feedback asymmetry with symmetric temperature profiles rather than symmetric CO₂ concentration profiles could provide a better quantification of asymmetry. In addition, the suitability of concentration-driven simulations for TCRE quantification is still in exploration. Using pulse emissions-driven simulations, Zickfeld et al. (2021) show evidence of compensation between the temperature and carbon cycle response, making the case for emissions-driven simulations rather than concentration-driven runs, that inhibit part of the climate-carbon cycle response. Further research should, therefore, focus primarily on improving quantification of TCRE asymmetry by running emissions-driven simulations with a more comprehensive earth system model that includes the full suite of physical climate feedbacks. Lastly, the robustness of these results should also be tested in a multi-model framework. Our work highlights the need to quantify metrics under negative emissions as reliance on metrics derived from positive emission scenarios may result in inaccurate quantification of the climate response under net negative CO₂ emissions.

6 Code and data availability

560 The UVic ESCM (University of Victoria Earth System Climate Model) data will be made available at <https://doi.org/10.5281/zenodo.17957657> upon acceptance, and the model code for UVic ESCM 2.10 is available at <http://terra.seos.uvic.ca/model/2.10/>.

7 Author contributions

KZ developed the research question. VRC ran the model simulations and worked with KZ to analyse and interpret the model 565 data and write the paper.

8 Competing interests

The contact author has declared that none of the authors has any competing interests.

9 Acknowledgements

Computing resources were provided by the Digital Research Alliance of Canada (formerly Compute Canada).

570



10 Financial support

This research has been supported by a Natural Sciences and Engineering Research Council of Canada (NSERC) Vanier Canada Graduate Scholarship (grant no. 182248).

575 11 References

Arora, V., Boer, G., Friedlingstein, P., Eby, M., Jones, C. D., Christian, J. R., Bonan, G., Bopp, L., Brovkin, V., Cadule, P., Hajima, T., Ilyina, T., Lindsay, K., Tjiputra, J. F., Wu, T.: Carbon-concentration and carbon-climate feedbacks in CMIP5 earth system models, *J. Clim.*, 26(15), 5289–5314, doi: 10.1175/JCLI-D-12-00494.1, 2013.

Arora, V. K., Katavouta, A., Williams, R. G., Jones, C. D., Brovkin, V., Friedlingstein, P., Schwinger, J., Bopp, L., Boucher, O., Cadule, P., Chamberlain, M. A., Christian, J. R., Delire, C., Fisher, R. A., Hajima, T., Ilyina, T., Joetzjer, E., Kawamiya, M., Koven, C. D., Krasting, J. P., Law, R. M., Lawrence, D. M., Lenton, A., Lindsay, K., Pongratz, J., Raddatz, T., Séférian, R., Tachiiri, K., Tjiputra, J. F., Wiltshire, A., Wu, T., and Ziehn, T.: Carbon–concentration and carbon–climate feedbacks in CMIP6 models and their comparison to CMIP5 models, *Biogeosciences*, 17, 4173–4222, doi.org/10.5194/bg-17-4173-2020, 2020.

Asaadi, A., Schwinger, J., Lee, H., Tjiputra, J., Arora, V., Séférian, R., Liddicoat, S., Hajima, T., Santana-Falcón, Y., & Jones, C. D.: Carbon cycle feedbacks in an idealized simulation and a scenario simulation of negative emissions in CMIP6 Earth system models, *Biogeosciences*, 21, 411–435, doi.org/10.5194/bg-21-411-2024, 2024.

Boer, G. J. and Arora, V.: Geographic Aspects of Temperature and Concentration Feedbacks in the Carbon Budget, *J. Clim.*, 23(3), 775–784, doi: 10.1175/2009JCLI3161.1, 2010.

Boucher, O., Halloran, P. R., Burke, E. J., Doutriaux-Boucher, M., Jones, C. D., Lowe, and Wu, P.: Reversibility in an earth system model in response to CO₂ concentration changes, *Environ. Res. Lett.*, 7, 024013, doi: 10.1088/1748-9326/7/2/024013, 2012.

Cao, L. and Caldeira, K.: Atmospheric carbon dioxide removal: Long term consequences and commitment, *Environ. Res. Lett.*, 5, 024011, 2010.

Chapin, F.S. and Eviner, V.T.: 10.6. Biogeochemical Interactions Governing Terrestrial Net Primary Production, In: Holland, H.D. and Turekian, K.K., Eds., *Treatise on Geochemistry*, 2nd Edition, Elsevier, Oxford, 189–216, doi.org/10.1016/B978-0-08-095975-7.00806-8, 2014.

Chimuka, V. R., Nzotungicimpaye, C.-M., and Zickfeld, K.: Quantifying land carbon cycle feedbacks under negative CO₂ emissions, *Biogeosciences*, 20, 2283–2299, doi.org/10.5194/bg-20-2283-2023, 2023, 2023.

Canadell, J.G., P.M.S. Monteiro, M.H. Costa, L. Cotrim da Cunha, P.M. Cox, A.V. Eliseev, S. Henson, M. Ishii, S. Jaccard, C. Koven, A. Lohila, P.K. Patra, S. Piao, J. Rogelj, S. Syampungani, S. Zaehle, and K. Zickfeld,: Global Carbon and other Biogeochemical Cycles and Feedbacks. In *Climate Change 2021: The Physical Science Basis. Contribution of Working Group I to the Sixth Assessment Report of the Intergovernmental Panel on Climate Change* [Masson-Delmotte, V., P. Zhai, A. Pirani,



S.L. Connors, C. Péan, S. Berger, N. Caud, Y. Chen, L. Goldfarb, M.I. Gomis, M. Huang, K. Leitzell, E. Lonnoy,
605 J.B.R. Matthews, T.K. Maycock, T. Waterfield, O. Yelekçi, R. Yu, and B. Zhou (eds.)], Cambridge University Press,
Cambridge, United Kingdom and New York, NY, USA, pp. 673–816, doi:10.1017/9781009157896.007, 2021.

Cox, P. M., Betts, R. A., Jones, C.D., Spall, S. A., and Totterdell, I.: Acceleration of global warming due to carbon-cycle
feedbacks in a coupled climate model, *Nature*, 408, 184–187, doi: 10.1038/35041539, 2000.

Cox, P. M., Betts, R. A., Collins, M., Harris, P. P., Huntingford, C., and Jones, C. D.: Amazonian forest dieback under climate-
610 carbon cycle projections for the 21st century, *Theor. Appl. Climatol.*, 78, 137–156, doi: 0.1007/s00704-004-0049-4, 2004.

Duan, Z. H. and Sun, R.: An improved model calculating CO₂ solubility in pure water and aqueous NaCl solutions from 273
to 533 K and from 0 to 2000 bar, *Chem. Geol.* 193, 257–271, 2003.

Eby, M., Weaver, A. J., Alexander, K., Zickfeld, K., Abe-Ouchi, A., Cimatoribus, A., ... and Zhao, F.: Historical and idealized
climate model experiments: An intercomparison of Earth system models of intermediate complexity, *Clim. Past*, 9(3), 1111–
615 1140, doi:10.5194/cp-9-1111-2013, 2013.

Ehlert, D., Zickfeld, K., Eby, M., and Gillett, N.: The sensitivity of the proportionality between temperature change and
cumulative CO₂ emissions to ocean mixing, *J. Climate*, 30, 2921–2935, doi: 10.1175/JCLI-D-16-0247.1, 2017.

Eyring, V., Bony, S., Meehl, G. A., Senior, C. A., Stevens, B., Stouffer, R. J. and Taylor, K. E.: Overview of the Coupled
Model Intercomparison Project Phase 6 (CMIP6) experimental design and organization, *Geosci. Model Dev.*, 9(5), 1937–
620 1958. doi:10.5194/gmd-9-1937-2016, 2016.

Friedlingstein, P., Cox, P. M., Betts, R. A., Bopp, L., Von Bloh, W., Brovkin, V., ...and Cadule, P.: Climate-carbon cycle
feedback analysis: Results from the C4MIP model intercomparison, *J. Clim.*, 19, 3337–3353., 2006.

Friedlingstein, P. and Prentice, I.: Carbon-climate feedbacks: A review of model and observation based estimates, *Curr. Opin.*
Environ. Sustainability, 2(4), 251–257, doi: 10.1016/j.cosust.2010.06.00, 2010.

Fung, I.Y., Doney, S. C., Lindsay, K., and Jasmin J. G.: Evolution of carbon sinks in a changing climate, *PNAS*, 102(32),
625 11201–11206, doi: 10.1073/pnas.0504949102, 2005.

Fuss, S., Lamb, W. F., Callaghan, M. W., Hilaire, J., Creutzig, F., Amann, T., ...and Minx, J. C.: Negative emissions—Part 2:
Costs, potentials and side effects, *Environ. Res. Lett.*, 13(6), 063002, doi.org/10.1088/1748-9326/aabf9f, 2018.

Gillett, N. P., Arora, V. K., Matthews, D., Allen, M. R.: Constraining the Ratio of Global Warming to Cumulative CO₂
630 Emissions Using CMIP5 Simulations, *J. Clim.*, 26, 6844–6858, doi.org/10.1175/JCLI-D-12-00476.1, 2013.

Gregory, J. M., Jones, C. D., Cadule, P., & Friedlingstein, P.: Quantifying carbon cycle feedbacks. *J. Clim.*, 22(19), 5232–
5250, doi: 10.1175/2009JCLI2949.1, 2009.

Jones, C. D., Ciais, J., Davis, S. J., Friedlingstein, P., Gasser, T., Peters, G. P. ... and Wiltshire, A.: Simulating the Earth System
response to negative emissions, *Environ. Res. Lett.*, 11, 095012, 2016.

Jones, C. D. and Friedlingstein, P.: Quantifying process-level uncertainty contributions to TCRE and carbon budgets for
635 meeting Paris Agreement climate targets, *Environ. Res. Lett.*, 15, 074019, doi.org/10.1088/1748-9326/ab858a, 2020.



Keller, D. P., Oschlies, A. and Eby, M.: A new marine ecosystem model for the University of Victoria earth system climate model, *Geosci. Model Dev.*, 5(5), 1195–1220, doi:10.5194/gmd-5-1195-2012, 2012.

640 Keller, D. P., Feng, E. Y., and Oschlies, A.: Potential climate engineering effectiveness and side effects during a high carbon dioxide-emission scenario, *Nat. Commun.* 5, 3304, <https://dx.doi.org/10.1038%2Fncomms4304>, 2014.

Koven, C. D., Arora, V. K., Cadule, P., Fisher, R. A., Jones, C. D., Lawrence, D. M. ... and Zickfeld, K.: Multicentury dynamics of the climate and carbon cycle under both high and net negative emissions scenarios, *Earth Syst. Dynam.*, 13, 885–909, doi.org/10.5194/esd-13-885-2022, 2022^a.

645 Koven, C. D., Sanderson, B. M., and Swann, A. L. S.: Much of the zero emissions commitment occurs before reaching net zero emissions, *Environ. Res. Lett.* 18, 014017, doi.org/10.1088/1748-9326/acab1a, 2022^b.

MacDougall, A. H. and Knutti, R.: Projecting the release of carbon from permafrost soils using a perturbed parameter ensemble modelling approach, *Biogeosciences*, 13(7), 2123–2136, doi:10.5194/bg-13-2123-2016, 2016.

Matthews, H., Gillett, N., Stott, P. and Zickfeld, K.: The proportionality of global warming to cumulative carbon emissions, *Nature*, 459, 829–832, doi.org/10.1038/nature08047, 2009.

650 Matthews, H. D., Landry, J.-S., Partanen, A.-I., Allen, M., Eby, M., Forster, P., ... and Zickfeld, K.: Estimating carbon budgets for ambitious mitigation targets, *Curr. Clim. Change Rep.*, 3(1), 69–77, doi.org/10.1007/s40641-017-0055-0, 2017.

Meissner, K. J., Weaver, A. J., Matthews, H. D. and Cox, P. M.: The role of land surface dynamics in glacial inception: a study with the UVic Earth System Model, *Clim. Dyn.*, 21(7–8), 515–537, doi:10.1007/s00382-003-0352-2, 2003.

655 Melnikova, I., Boucher, O., Cadule, P., Ciais, P., Gasser, T., Quilcaille, Y. ... and Tanaka, K.: Carbon cycle response to temperature overshoot beyond 2°C: An analysis of CMIP6 models, *Earth's Future*, 9, e2020EF001967, doi.org/10.1029/2020EF001967, 2021.

Mengis, N., Keller, D. P., MacDougall, A., Eby, M., Wright, N., Meissner, K. J. ... and Zickfeld, K.: Evaluation of the University of Victoria Earth System Climate Model version 2.10 (UVic ESCM 2.10), *Geosci. Model Dev. Discuss.*, 1–28, 2020.

660 Pacanowski, R. C.: MOM 2 Documentation, users guide and reference manual, GFDL Ocean Group Technical Report 3, Geophys. Fluid Dyn. Lab., Princeton Univ. Princeton, NJ, 195.

Paustian, K., Lehmann, J., Ogle, S., Reay, D., Robertson, G. P., & Smith, P.: Climate-smart soils, *Nature*, 532, 49–57, doi.org/10.1038/nature17174, 2016.

Powis, C. M., Smith, S. M., Minx, J. C., and Gasser, T.: Quantifying global carbon dioxide removal deployment, *Environ. Res. Lett.*, 18(2), 024022, 2023.

665 Sanderson, B. M., Booth, B. B. B., Dunne, J., Eyring, V., Fisher, R. A., Friedlingstein, P., Gidden, M. J., Hajima, T., Jones, C. D., Jones, C. G., King, A., Koven, C. D., Lawrence, D. M., Lowe, J., Mengis, N., Peters, G. P., Rogelj, J., Smith, C., Snyder, A. C., Simpson, I. R., Swann, A. L. S., Tebaldi, C., Ilyina, T., Schleussner, C.-F., Séférian, R., Samset, B. H., van Vuuren, D., and Zaehle, S.: The need for carbon-emissions-driven climate projections in CMIP7, *Geosci. Model Dev.*, 17, 8141–8172.

670 doi.org/10.5194/gmd-17-8141-2024, 2024.



Sanderson, B. M., Brovkin, V., Fisher, R. A., Hohn, D., Ilyina, T., Jones, C. D., Koenigk, T., Koven, C., Li, H., Lawrence, D. M., Lawrence, P., Liddicoat, S., MacDougall, A. H., Mengis, N., Nicholls, Z., O'Rourke, E., Romanou, A., Sandstad, M., Schwinger, J., Séférian, R., Sentman, L. T., Simpson, I. R., Smith, C., Steinert, N. J., Swann, A. L. S., Tjiputra, J., and Ziehn, T.: flat10MIP: an emissions-driven experiment to diagnose the climate response to positive, zero and negative CO₂ emissions, 675 Geosci. Model Dev., 18, 5699–5724. doi.org/10.5194/gmd-18-5699-2025, 2025.

Schwinger, J., and Tjiputra, J. F.: Ocean carbon cycle feedbacks under negative emissions, Geophys. Res. Lett., 45(10), 5062-5070, doi: 10.1029/2018GL077790, 2018.

Smith, P., Davis, S. J., Creutzig, F., Fuss, S., Minx, J., Gabrielle, B., ...and Yongsung, C.: Biophysical and economic limits to negative CO₂ emissions, Nature Climate Change, 6(1), 1-9, 2015.

680 Smith, S. M., Geden, O., Nemet, G., Gidden, M., Lamb, W. F., Powis, C., Bellamy, R., Callaghan, M., Cowie, A., Cox, E., Fuss, S., Gasser, T., Grassi, G., Greene, J., Lück, S., Mohan, A., Müller-Hansen, F., Peters, G., Pratama, Y., Repke, T., Riahi, K., Schenuit, F., Steinhauser, J., Strefler, J., Valenzuela, J. M., and Minx, J. C.: The State of Carbon Dioxide Removal – 1st Edition, The State of Carbon Dioxide Removal, doi.org/10.17605/OSF.IO/W3B4Z, 2023.

Tokarska, K. B. and Zickfeld, K.: The effectiveness of net negative carbon dioxide emissions in reversing anthropogenic 685 climate change, Environ. Res. Lett., 094013, 2015.

UNFCCC (2015). Adoption of the Paris Agreement. Retrieved from <https://unfccc.int/sites/default/files/resource/docs/2015/cop21/eng/109r01.pdf>

Weaver, A. J., Eby, M., Wiebe, E. C., Bitz, C. M., Duffy, P. B., Ewen, T. L., ... and Fanning, A. F.: The UVic Earth System Climate Model: Model description, climatology, and applications to past, present and future climates, Atmosphere Ocean, 39, 690 361-428, 2001.

Zickfeld, K., Eby, M., Matthews, H. D., Schmittner, A., and Weaver, A. J.: Nonlinearity of carbon cycle feedbacks, J. Clim., 24(16), 4255-4275, doi: 10.1175/2011JCLI3898.1, 2011.

Zickfeld, K., MacDougall, A. H., and Matthews, H. D.: On the proportionality between global temperature change and cumulative CO₂ emissions during periods of net negative CO₂ emissions, Environ. Res. Lett., 11(5), 055006, 695 doi.org/10.1088/1748-9326/11/5/055006, 2016.

Zickfeld, K., Azevedo, D., Mathesius, S., and Matthews, H. D.: Asymmetry in the climate–carbon cycle response to positive and negative CO₂ emissions. Nat Clim. Change, 11, 613-617, doi.org/10.1038/s41558-021-01061-2, 2021.